3.1 About project B6 (E)

3.1.1 Title: Parvovirus B19 and Endothelial Regeneration – Therapeutic Perspectives

3.1.2 Principal investigators

Schmidt-Lucke, Caroline, Priv.-Doz. Dr. med., born 30.03.1968, German
Charité – Universitätsmedizin Berlin, Medizinische Klinik II, Campus Benjamin Franklin, CharitéCentrum 11 Herz- und Kreislauf- und Gefäßmedizin, Hindenburgdamm 30,
12200 Berlin, Germany
Phone +49 30 8445 2288, Email: caroline.schmidt-lucke@charite.de

Tschöpe, Carsten, Prof. Dr. med., born 20.08.1963, German
Charité – Universitätsmedizin Berlin, Medizinische Klinik II, Campus Benjamin Franklin, CharitéCentrum 11 Herz- und Kreislauf- und Gefäßmedizin, Hindenburgdamm 30,
12200 Berlin, Germany
Phone +49 30 8445 4780, Email: carsten.tschoepe@charite.de

Fechner, Henry, Dr. med. vet., born 23.06.1965, German
Technische Universität Berlin, Institut für Biotechnologie, TIB 4/3-2, Fachgebiet Angewandte Biochemie, Gustav-Meyer-Allee 25, 13355 Berlin, Germany
Phone:+49 30 314 72181
Email: henry.fechner@tu-berlin.de

3.2 Project history

3.2.1 Report

Mechanisms of injury are unclear in patients with chronic parvovirus B19 (B19V)-associated organ damage. According to current knowledge, only erythroid progenitor cells (ErPC) permit replication and persistence of B19V. A heterogenous group of bone marrow-derived circulating angiogenic cells (CAC) plays an indispensable role in the repair of damaged endothelium as prerequisite for organ function. Owing to the strong kinship of erythropoiesis and cells participating in vasculogenesis, CAC as targets in B19V-induced endothelial damage come to the fore.

We tested the hypothesis that B19V directly infects CAC and interferes with their endothelial regenerative potential. Against primary expectation, patients with chronic B19V cardiomyopathy present with systemic endothelial cell (EC) apoptosis. In patients with B19V-cardiomyopathy, highest concentrations of B19V DNA were found in the $CD34^+KDR^+$-PC fraction compared to haematopoetic progenitors and lineage committed cells ($p<0.05$). Indicating B19V replication, B19V mRNA was found in angiogenic progenitor cells in the majority of these patients. Significantly reduced numbers of eo-EPC ($p<0.05$) indicate dysfunctional cellular endothelial regeneration in these patients. CAC present the necessary receptor status for B19V attachment and internalisation with consequent virus uptake. Detection of late B19V genes after infection in CAC, restricted to at least semi-permissive cell types, further tags these cells as novel objects for B19V infection. Expression of the viral proteins resulted in caspase-8 and caspase-10 dependent induction of apoptosis. We demonstrate CAC as targets for infection by B19V and causative agent for impaired endothelial regenerative capacity, thus challenging the established concept of B19V being responsible for a primary chronic organ disease.

It was the aim of the previous funding period to work out a link between B19V infection and causal impairment of endothelial regeneration. **We had four hypotheses**:

1. There is a systemic, rather than a local cardiac induction of endothelial apoptosis and cardiac homing of CAC
2. B19V replicates in CAC of bone marrow with dissemination of infected CAC in B19V-cardiomyopathy
3. B19V-infection is associated with CAC dysfunction
4. Indirect, immunological mediated mechanisms play a role in EC damage

We investigated whether interferon-ß (IFN-ß) reduced endothelial damage in patients with cardiac persistence of B19V in a phase-I study.

In vitro, B19V infected cultivated endothelial cells (EC) and lead to a reduction of their viability (p=0.007). IFN-ß suppressed B19V replication by 63% (p=0.008) in EC and increased their viability (p=0.021). Circulating mature apoptotic EC (CMAEC; $CD45^{-}CD146^{+}vWF^{+}annexin\text{-}V^{+}$) and angiogentic cells (CAC; $CD34^{+}KDR^{+}$) were quantified with FACS in 9 symptomatic patients with cardiac B19V before and after 6 months of 16 MioU IFN-ß therapy compared to 9 healthy controls (Figure 1 A and B). Endothelial dysfunction was measured using flow-mediated dilatation (FMD) of the forearm. Patients with B19V had significantly higher (p = 0.004) levels of CMAEC vs. controls, that normalised after treatment (0.06±0.08% vs. 0.01±0.006%, p=0.008). Similar improvement was shown for FMD (p=0.04) in the treatment group only (vs. untreated patients with B19V (n = 5), p=0.017). There were significantly higher numbers of CAC in patients with B19V before therapy (0.04±0.05 vs. 0.01± 0.004; p=0.02) compared to control subjects, that normalised after treatment (p=0.03).

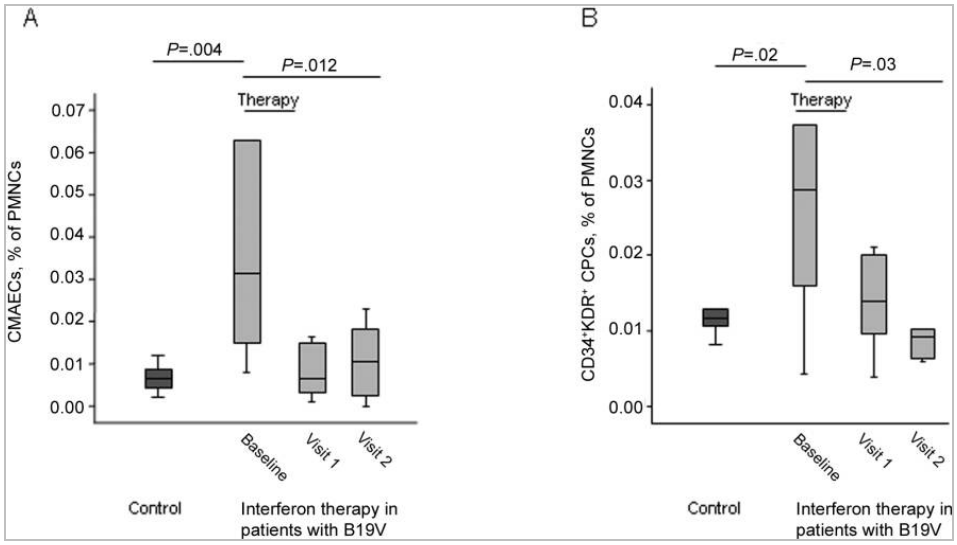

Figure 1. Percentage of circulating mature apoptotic endothelial cells (CMAECs) (A) and of circulating CD34+KDR+ progenitor cells (CAC) (B) among peripheral mononuclear cells (PMNCs) in 9 control subjects and in 9 patients with human parvovirus B19 (B19V) persistence before and after a 6- month course of interferon beta therapy. Significance levels are given for group comparisons and for changes in patients during interferon beta therapy. The horizontal line in the middle of each box indicates the median; the top and bottom borders of the box mark the 75th and 25th percentiles, respectively; and the whiskers above and below the box mark the range.

Thus, for the first time we show modulation of virus-induced chronic endothelial damage, specifically, endothelial cell apoptosis and endothelial regeneration.

In 17 patients presenting with chronic B19V-positive cardiomyopathy, B19V DNA and its replication intermediates, B19V mRNA, were isolated from endomyocardial biopsies, bone marrow and circulating $CD34^{+}KDR^{+}$ angiogenetic progenitor cells (PC). Numbers of eo-EPC were quantified and compared to healthy controls. In patients with B19V-cardiomyopathy, highest concentrations of B19V DNA were found in the $CD34^{+}KDR^{+}$-PC fraction compared to haematopoetic progenitors and lineage committed cells (Fig. 2A, p<0.05). Indicating B19V replication, B19V mRNA was found in angiogenic progenitor cells the majority of these patients. The necessary receptor status for B19V-infection is present on $CD34^{+}KDR^{+}$-PC. Significantly reduced numbers of eo-EPC (Fig. 2 C and D, p<0.05) indicate dysfunctional cellular endothelial regeneration in these patients.

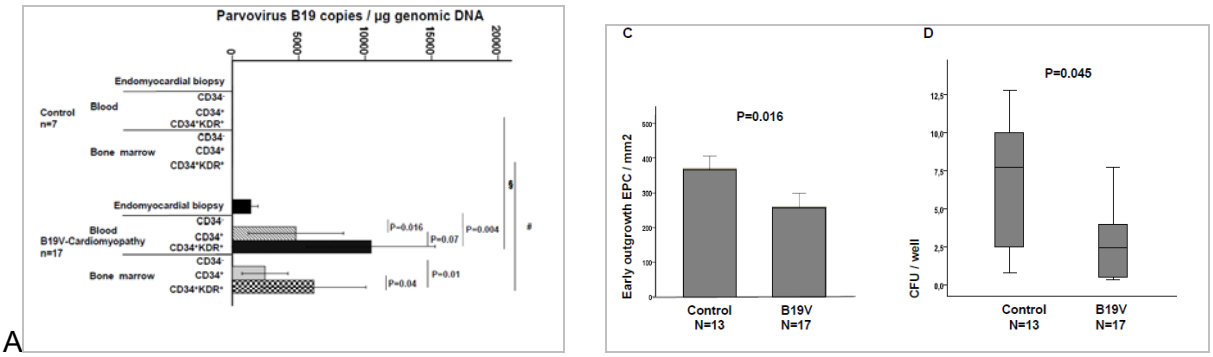

Figure 2: A, Erhöhte Quantification of Parvovirus B19 DNA of endomyocardial biopsy and different cell fractions from patients with B19V-associated cardiomyopathy compared to controls with a previous unnoticed B19V infection. B19V DNA related to µg genomic DNA was significantly ($p<0.05$) increased in patients with B19V (n=10) compared to controls (n=7) in magnetically separated circulating progenitor cells (CPC, $CD34^+KDR^+$), haematopoietic progenitor cells ($CD34^+$) and lineage committed cell fraction ($CD34^-$) from blood and bone marrow. P-values relate to intraindividual differences between the cell fractions $CD34^-$, $CD34^+$, and $CD34^+KDR^+$. § indicates CPC B19V vs. control: p=0.025, # indicates BM-PC B19V vs. control: p=0.014, bars represent mean and SE. C, Numbers of cultivated early outgrowth EPC characterised by the uptake of the uptake of 1,19–dioctadecyl–3,3,39,39–tetramethylindocarbocyanine–labeled acetylated low-density lipoprotein (DiLDL) and (D) of CFU Hill are significantly reduced in patients with B19V compared to controls.

Thus, infection and replication of B19V in circulating angiogenetic cells and consequent dysfunctional endogenous vascular repair support a primary bone marrow disease underlying secondary cardiomyopathy.

In a clinical study of patients with chronic B19V-cardiomyopathy, with elevated systemic levels of CMAEC, no transcardiac increase of CMAEC was found. In contrast, patients with acute coronary syndromes show elevated systemic EC apoptosis to controls (ACS: 8.7 ± 7.5 versus healthy controls 2.7 ± 3.6 CMAEC / µl peripheral blood, $P < 0.05$, data not shown) and, additionally, local cardiac activation of EC apoptosis (Fig. 3). This finding points towards the systemic nature of B19V induced endothelial apoptosis, challenging the concept of a primarily cardiac endothelial damage.

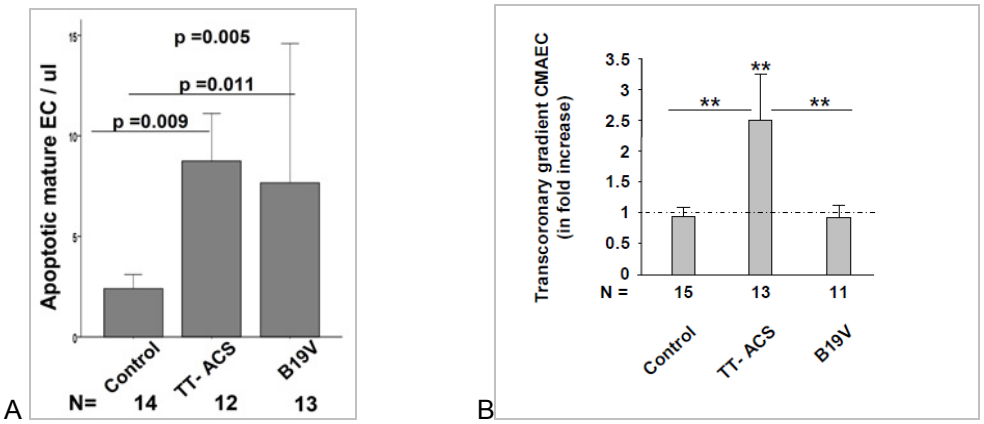

Figure 3: A, Systemic absolute values of CMAEC ($CD45^-CD146^+vWF^+Annexin\ V^+$). B, Transcoronary gradients as indicated by the changes of samples taken from the great cardiac vein compared to the systemic circulation. Fold increase of CMAEC in 15 healthy controls, 13 patients with troponin T-negative acute coronary syndromes (ACS; Braunwald IIIB) and 11 patients with chronic B19V-cardiomyopathy, compared to the individual systemic values, set as 1. Bars represent mean changes from baseline, defined as values taken from aortic root + SD. Transcoronary increase of CMAEC is found in patients with unstable angina (P = 0.01–0.005 for paired comparison, P = 0.05–0.01 against control or patients with B19V-cardiomyopathy, P < 0.05 for trend (ANOVA).

The necessary cellular receptor P antigen and the coreceptors ß1-integrin and Ku80 showed ample presence on CAC as comparable to the semi-permissive cell line UT7/Epo-S1 (Fig. 4A). Higher expression of the P-antigen was detected compared to mature EC. To prove intracellular presence of B19V, nucleic acids were quantified by *in situ* hybridization analysis (ISH) after *in vitro* infection of CAC with B19V using a probe detecting B19V genomes and viral transcripts (Fig. 4B). As positive controls, 65% of UT7/Epo-S1 stained B19V positive (Fig. 4C). Comparable B19V infection was proven for eo-EPC, ECFC and to a lesser extent for CFU-Hill cells. HeLa cells, as negative control, showed no infection. Eo-EPC showed the highest rate of infected cells 24 h post infection (p.i.) (68%) with a

further increase 72 h p.i. (93%) compared to other CAC and UT7/Epo-S1 cells. The time-dependent increase of B19V infected eo-EPC suggests viral transcription or even, replication. After 72 hours, only small numbers of ECFC, with considerable less infected cells were present, giving rise to the hypothesis of high cell damage with consequent detachment. Due to the low infection rate of CFU-Hill colonies and their cellular heterogeneity, further experiments were pursued only with eo-EPC and ECFC. Immunofluorescence microscopy detected B19V capsid proteins in eo-EPC and ECFC. Furthermore, nuclear viral particles of around 26 nm size were observed 48 h p.i. of eo-EPC by transmission electron microscopy (Fig. 4D) in regions of condensed chromatin. The early non-structural protein NS1 could be readily detected 24 h p.i. in ECFC with a further increase 48 h p.i. (Fig. 4E). Furthermore, expression of B19V late 11kDa and VP1/VP2 transcripts 24 h p.i. in ECFC yield a hint for viral replication. As demonstrated for erythroid progenitor cells (Chen, J Virol. 2011) hypoxia further increased NS1 mRNA expression.

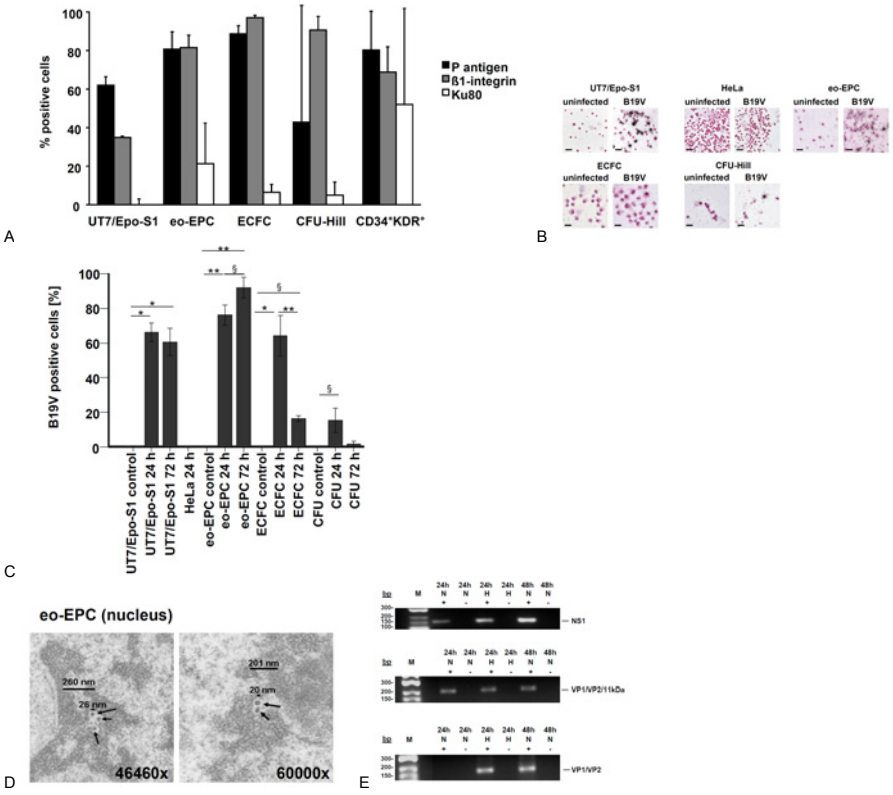

*Figure 4: A, UT7/Epo-S1 and CAC were stained with antibodies for the B19V receptor blood group P antigen and the co-receptors ß1-integrin and Ku80, followed by flow cytometry analysis. The semi-permissive megakaryoblastoid cell line UT7/Epo-S1 served as a positive control.. (B+C) In situ hybridization analysis (ISH) and quantification of B19V infected CAC. UT7/Epo-S1 and HeLa cells served as positive and negative control, respectively. Eo-EPC, CFU-Hill and ECFC were infected with purified B19V. ISH was performed using a ^{35}S labelled probe detecting B19V DNA and RNA. Cells were counterstained with HE. (B) Representative pictures shown from cells 24 h p.i. (scale bar: 50 µm). (C) B19V positive cells were determined by counting positive grains in each cell. The mean value of grains per cell of the respective uninfected control ± 3 times SD was set as background. Values higher than background defined B19V positive cells. Statistical significance compared to controls is shown for P < 0.1 by §, for P < 0.05 by * and for P < 0.01 by ** (Mann-Whitney test). Data are means ± SD. (D) Electron microscopy of B19V infected eo-EPC. Ultra-thin 70 nm sections were analyzed by transmission electron microscopy. Viral particles were detected in nuclei at magnifications of 46,460x and 60,000x. (E) B19V early and late transcripts are synthesized in in vitro infected ECFC. Total RNA was isolated from in vitro infected ECFC 24 and 48 h p.i. under normoxic or hypoxic conditions for RT-PCR. +: reverse transcribed cDNA, -: RNA without reverse transcription, N: normoxia, H: hypoxia.*

Regardless of the cell's capacity to replicate B19V, accumulation of B19V NS1 and 11kDa proteins have been shown to directly induce apoptosis in different non-permissive and permissive cell lines[32]. Induction of apoptosis through the B19V 11kDa protein involves the death receptor signalling pathway and initiator caspase-8 and -10 in erythroid cell lines[32]. Both, eo-EPC and ECFC, showed a strong activation of caspase-3 (Fig. 5A) and binding of annexin V (Fig. 5B) 24 h p.i. This finding was

confirmed by a TUNEL assay detecting terminal apoptosis after B19V infection of eo-EPC and ECFC (Fig. 5C). Stress by hypoxic conditions in eo-EPC, simulating conditions in the bone marrow, increased numbers of TUNEL+ cells 3.5-fold ($P < 0.01$, data not shown) compared to normoxia. Likewise, numbers of TUNEL+ eo-EPC increased time-dependently 2.5-fold from 24 h to 72 h p.i. ($P < 0.005$, data not shown). In contrast, no apoptosis was induced in non-adherent cells, present in the same well as the adherent eo-EPC, indicating specificity of B19V infection (Fig. 5C). The individual contribution of NS1, 11kDa, and the capsid proteins VP1 and VP2 to the induction of apoptosis in CAC was dissected by transfection with the respective expression plasmids. Due to restrictions in liposomal transfection efficiency of eo-EPC (data not shown), experiments were carried out with ECFC only. Liposomal transfection of a reporter plasmid resulted in 21% GFP positive ECFC. Induction of apoptosis was measured by annexin V and active caspase-3 staining 24 h post transfection. NS1, 11kDa and VP1 led to a nearly identical, strong activation of caspase-3 (Fig. 5D) and annexin V staining (Fig. 5E), thus implying a novel role for VP1, and to a lesser extent for VP2, in apoptosis induction. The 11kDa protein showed the highest induction of annexin V positive cells (45%) compared to NS1 and VP1 (35%), thus outnumbering the amount of transfected cells. To dissect the mechanism of apoptosis induction in CAC, we performed a preincubation experiment with a mixture of caspase-8 and -10 peptide inhibitors. Indeed, simultaneous inhibition of caspase-8 and -10 led to a dose-dependent inhibition of apoptosis in eo-EPC and ECFC. Individual caspase inhibitors demonstrated a primary role for caspase-8 (Fig. 5F) with a higher inhibition of apoptosis compared to caspase-10 in both, eo-EPC and ECFC (both $P < 0.01$).

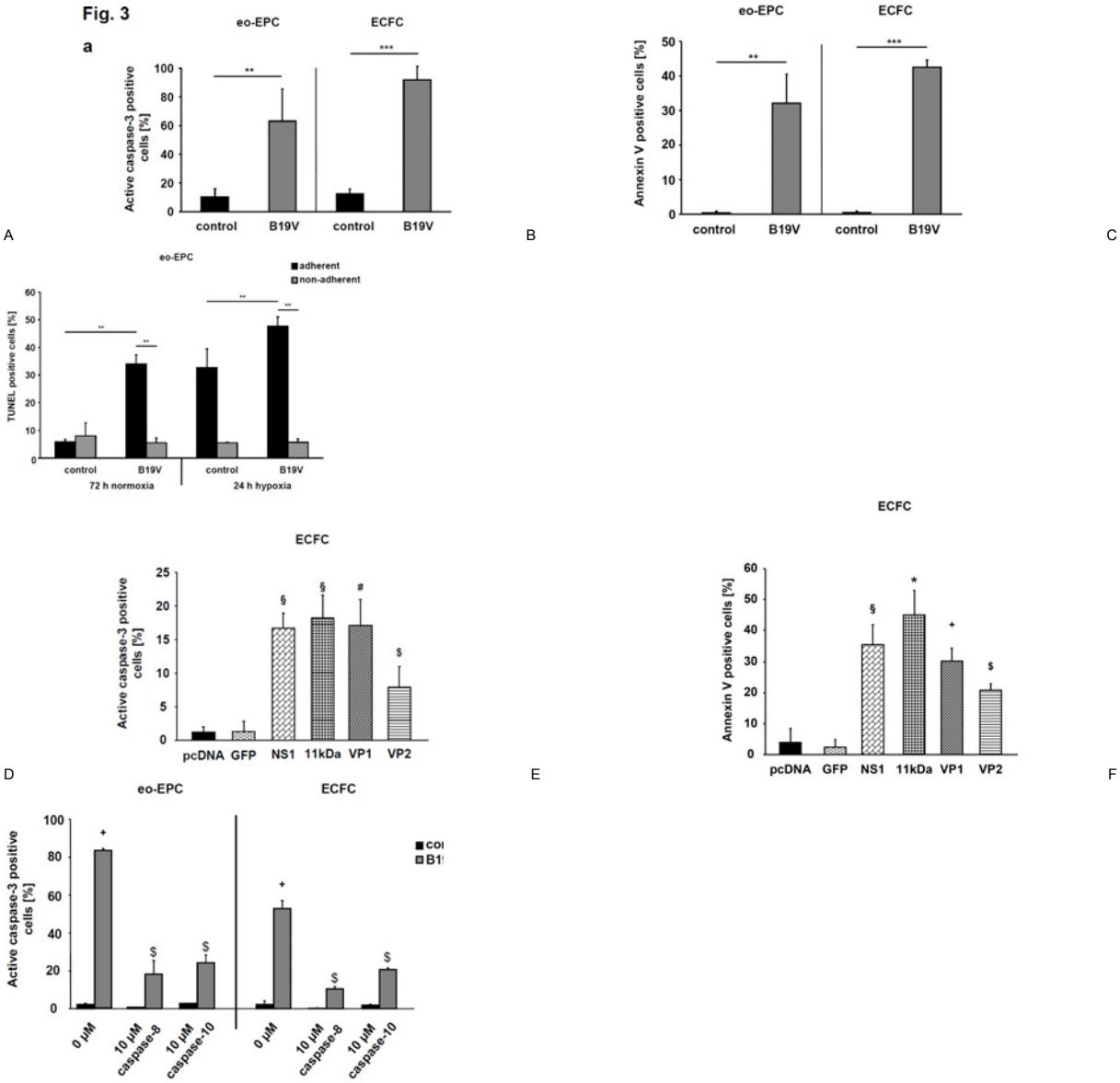

Figure 5: (A+B) Induction of apoptosis was quantified in B19V infected or control eo-EPC and ECFC through binding of annexin V-FITC (A) or an anti-active caspase-3 antibody (B) 24 h p.i. (C) TUNEL assay of B19V

*infected or control eo-EPC was performed under normoxic and hypoxic conditions at indicated time points post-infection. Adherent and non-adherent cells were stained. (D+E) Caspase-3 activation (D) and binding of annexin V (E) 24 h post-transfection with B19V NS1, 11kDa, VP1 and VP2 in ECFC. Plasmids pcDNA and pcDNA-GFP served as controls. P < 0.001 vs. control and VP2 indicated by §, P < 0.001 vs. control and P = 0.001–0.09 vs. VP2 by #, P < 0.001 vs. control, NS1, 11kDa, and VP1 by $, P < 0.001 vs. control and 11kDa and P = 0.001–0.09 vs. VP2 by +, P < 0.001 vs. control, VP1 and VP2 and P = 0.001–0.09 vs. NS1 by *.*
(F) Reduction of apoptosis with caspase-8 vs. caspase-10-inhibitor. Eo-EPC and ECFC were treated with indicated amounts of individual caspase-8 and -10 inhibitors before infection. Dimethyl sulfoxide (DMSO) served as control by supplementing each experiment to the highest concentration. P < 0.05 for trend (ANOVA), + indicates P < 0.001 vs. control, $ indicates P < 0.001 vs. control and uninhibited , # indicates P < 0.001 vs. uninhibited and 10µM. Data are means ± SD.

Since B19V is strictly pathogenic to human cells, we proved a detrimental effect of B19V on endothelial regenerative capacity by transplantation of B19V infected human eo-EPC after a carotid injury in immunodeficient SCID beige mice. Transplantation of B19V infected eo-EPC resulted in a significantly 2.4-fold reduced area of reendothelialisation compared to control eo-EPC (Fig. 6 A), illustrating reduced regenerative capacity after B19V infection *in vivo*. Consecutively, murine blood and bone marrow progenitor cells with endothelial regenerative potential, double stained with the mouse stem cell markers c-kit (CD117) and FLK-1 (CD309), were quantified. Numbers of c-kit$^+$FLK-1$^+$ cells significantly increased in both, bone marrow (17.4-fold) and blood (9-fold) of B19V infected cell transplanted mice compared to plasma controls (Fig. 6 B), thus reflecting endogenous proliferation and mobilisation. B19V causally impaired endothelial regeneration with trafficking of B19V in CAC in the animal model *in vivo*.
In contrast to sham treated animals, human cells were found attached to the denuded vessels after transplantation of eo-EPC. Indicating that, indeed, B19V is carried to the damaged vessel walls, we demonstrated B19V-infected human eo-EPC in the murine carotis (Figure 6c)

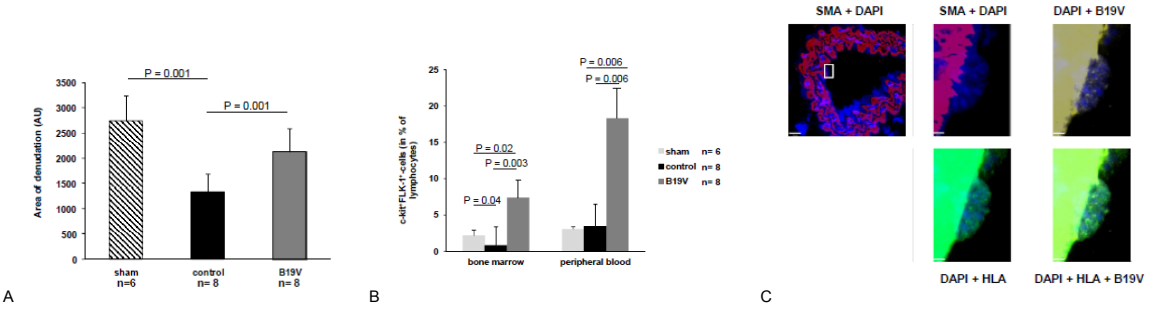

Figure 6: (A) Reendothelialisation of a carotid artery injury in male SCID beige mice after sham treatment, or injection of human non-infected (control) and B19V-infected eo-EPC. Quantification was performed three days after cell injection by Evans Blue staining. Mean values of denuded area are shown in arbitrary units (AU). Data are mean + SD. p<0.001 for trend in multivariate analysis.
(B) FACS analysis of bone marrow and peripheral blood mononuclear cells double-stained with CD117 (c-kit) and CD309 (flk-1) antibodies from mice after sham treatment, or injection of human non-infected (control) and B19V-infected eo-EPC. Data are mean + SD.
C) Multicolor-immunofluorescence imaging of murine carotis cross sections detecting human B19V-infected eo-EPC in the denuded area at day 3. Blue. DAPI; red: SMA; green: HLA-I; yellow: B19V; bars represent 17 µm (left, overview) and 2.6 µm (right, detail sections).

Our results show that the vasculotropic B19V infects bone marrow-derived CAC and has an impact on endogenous endothelial regeneration capacity, thus providing a novel pathogenetic approach for B19V-associated cardiac damage and persistence. B19V cardiomyopathy may represent an illustrative example for the proposed mode of *chronic* B19V vascular disease. Finally, proving a causal relation on dysfunctional endothelial regenerative capacity *in vivo*, experimental reendothelialisation was significantly reduced with B19V infected eo-EPC. This was despite proliferation and mobilisation of endogenous c-kit$^+$flk-1$^+$-progenitor cells as a compensatory effect, resembling the analogous finding of increased numbers of CAC in patients with chronic B19V infection [26]. Presence of human B19V-infected eo-EPC attached to damaged murine vessels indicates a possible mechanism of viral dissemination through cellular transport.

Increased numbers of CAC may derive from disruption of the CXCR4 /SDF-1 axis essential for mobilisation from bone marrow and recruitment into tissues. We therefore tested the hypothesis that B19V has the potential to interfere with the trafficking of CAC.
Reproducing our similar results, there were significantly higher numbers of $CD45^{dim}CD34^{+}KDR^{+}$-PC in patients with B19V-cardiomyopathy compared to controls. Similarly, the more premature subset of CAC, characterised by the coexpression of CD133 and KDR, was significantly increased in patients with B19V cardiomyopathy (Figure 7A). To analyse whether increased numbers of circulating CAC were attributable to enhanced mobilisation, serum SDF-1α levels were quantified. Patients with B19V-cardiomyopathy had significantly higher SDF-1α levels (Figure 7B). To examine whether the marker IP-10, known to parallel viral diseases and end-organ damage, would identify this cohort with ongoing inflammatory disease, circulating IP-10 levels were compared to controls. IP-10 was significantly elevated in B19V-patients (Figure 7C). Lower surface expression of CXCR4 on CAC postulates longer prolonged dwelling of these cells in the circulation with impaired homing capacity (Figure 7D). Thus, both increased mobilisation and impaired homing of CAC with dysfunctional properties may contribute of the increased numbers of CAC.

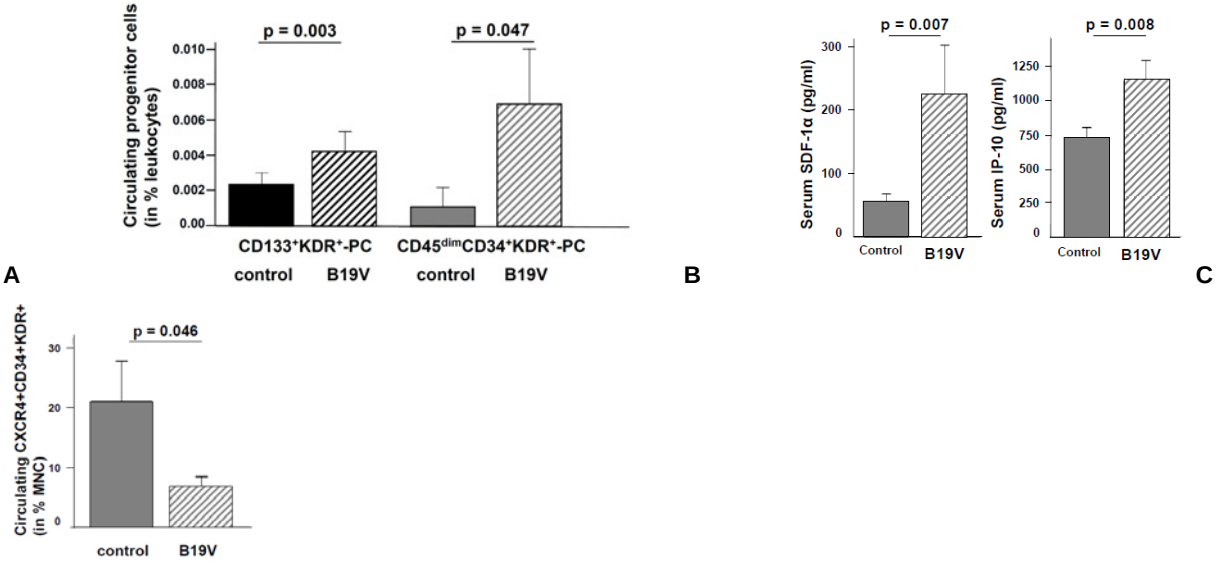

Figure 7: (A - D) CAC and in patients with B19V-cardiomyopathy compared to controls. A, Quantification of circulating endothelial progenitor cells ($CD133^{+}KDR^{+}$ and $CD45^{dim}CD34^{+}KDR^{+}$). B, Serum levels of SDF-1a. C, Serum levels of IP-10. D, Surface expression of CXCR4 on CAC. Data present the values as average + SD.

To examine a contributing effect of $CD45^{dim}CD34^{+}KDR^{+}$-PC to cardiovascular regeneration, transcardiac gradients were measured through simultaneously sampling of blood from the aorta and coronary sinus. In contrast to controls, only in patients with B19V-cardiomyopathy, a transcoronary reduction of $CD45^{dim}CD34^{+}KDR^{+}$-PC of – 47% (Figure 8A) was observed in the great cardiac vein compared to aorta. Consistently, SDF-1α mRNA concentration from endomyocardial biopsies was elevated in these patients (Figure 8B), indicating homing and retention of these cells. On the other side, we cannot exclude, that these cells experience an adverse fate. There was a significant correlation between numbers of $CD45^{dim}CD34^{+}KDR^{+}$-PC and SDF-1α mRNA in EMB (r = 0.48, p = 0.026, not shown). Expectedly, SDF-1α and HIF-1α mRNA correlated significantly (r = 0.51, p = 0.012, not shown), indicating ischaemia-triggered increase of SDF-1α.

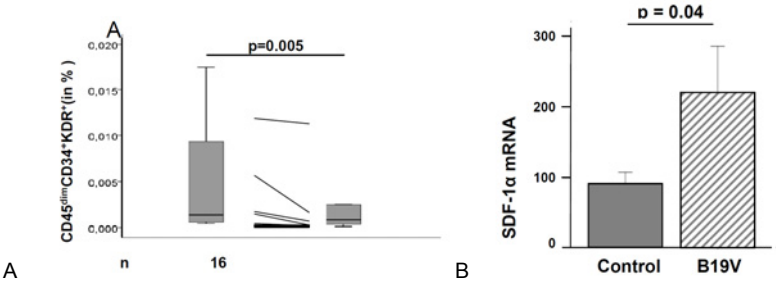

Figure 8: A, Quantitative analysis of transcardiac gradients of $CD45^{dim}CD34^{+}KDR^{+}$ in patients with B19V-cardiomyo-pathy. B, Quantification of SDF-1a mRNA from endomyocardial biopsies from patients with B19V-cardiomyopathy compared to controls

We have previously shown cellular transcardiac gradients in transplant vasculopathy. Currently, the effect of B19V infection and transfection with the B19V-components are being evaluated to dissect indirect versus direct effects on CXCR4 expression. Furthermore, vascular density and quantification of cardiac progenitor cells from endomyocardial biopsies of this patient cohort is undertaken.

Preliminary data show, that infection of ECFC with B19V has a profound effect on the angiogenetic profile. Specifically, in addition to gene expression involving mitochondrial function, differentiation (Notch) and the death receptor, B19V infection of CAC modulates G1S, HIF-1a, NO, PTEN, VEGF. The latter have been shown to be candidates for mi-RNA-21. Consecutive experiments are currently undertaken.

Treatment with telbivudine, a synthetic thymidine nucleoside analogue, has been shown to reduce B19V load and improve clinical symptoms in B19V-cardiomyopathy (Z1).

We first studied the necessary receptor and co-receptor status for B19V infection in CAC and the semi-permissive megakaryoblastoid cell line UT7/Epo-S1, as positive controls. Interestingly, pre-treatment of CAC with Telbivudine resulted in a significant increase of the B19V receptor and co-receptor status in the different cell types (eo-EPC (n = 4): P-antigen: 19%, ß1-integrin: 14%, KU80: 32%; ECFC (n = 3): P-antigen: 24%, ß1-integrin: 18%, KU80: 60%; UT7/Epo-S1 cells (n = 4): P-antigen: 25%, ß1-Integrin: 32%, KU80: 26%) compared to untreated controls.

We have previously shown a strong induction of apoptosis in CAC induced through the B19V NS1 and 11kDa. Having shown an increase of B19V transcripts in the early acute B19V infection in response to Telbivudine, we assessed the magnitude of apoptosis in CAC under this condition. Surprisingly, pretreatment with Telbivudine significantly ($p<0.001$) reduced the B19V-induced apoptosis, as measured by activation of the effector caspase-3 in ECFC (B19V –Telbivudine 81.5 ± 11.7% vs. B19V +Telbivudine 45.8 ± 19.3% active caspase-3 positive cells compared to control –Telbivudine 3.3 ± 2.4% vs. control +Telbivudine 1.8 ± 1.3%) eo-EPC (B19V –Telbivudine 51.8 ± 2.3% vs. B19V +Telbivudine 31.0 ± 5.6% active caspase-3 positive cells compared to control –Telbivudine 4.1 ± 1.7% vs. control +Telbivudine 1.6 ± 0.4%).

To further dissect the mechanism of B19V in inducing apoptosis, we analysed multiple pathways through a PCR array for human apoptosis. Infection of ECFC with B19V let to a strong down regulation of BIRC3 (CIAP-2) mRNA levels. Treatment of CAC with Telbivudine prior to B19V infection reversed this effect. This was confirmed by Single PCR ($p = 0.017$) and Western blot analysis.

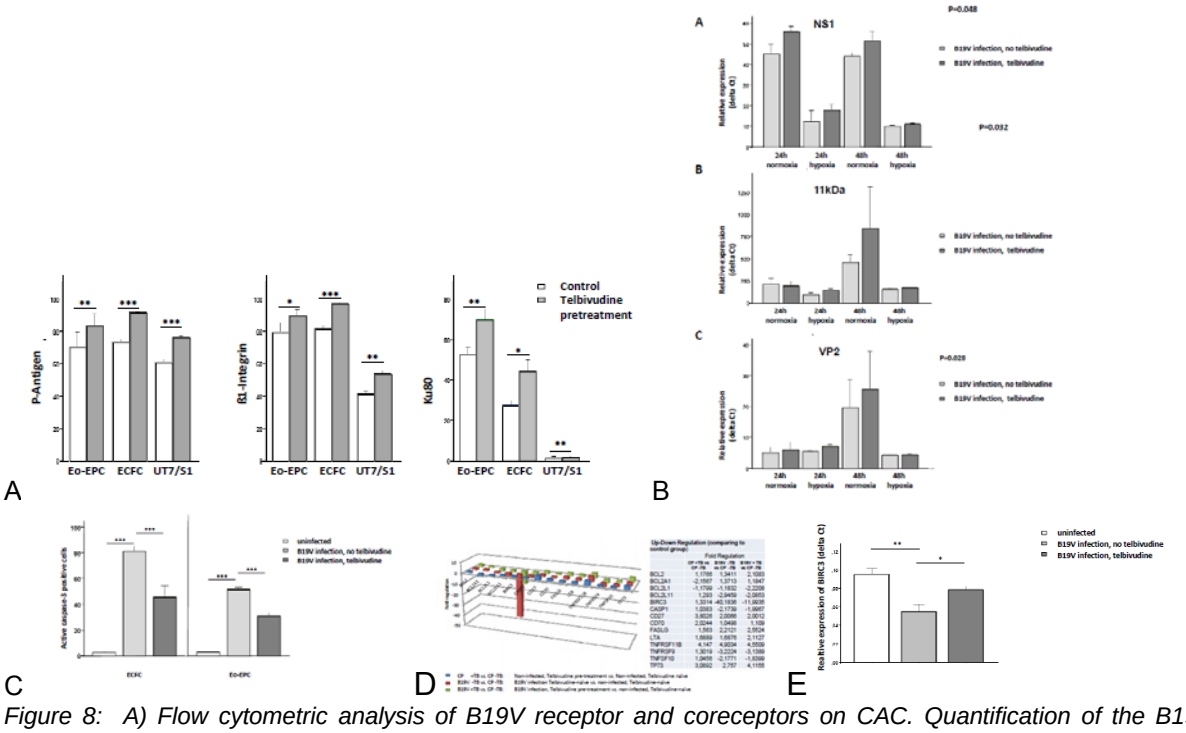

Figure 8: A) Flow cytometric analysis of B19V receptor and coreceptors on CAC. Quantification of the B19V (receptor P antigen and the coreceptors ß1-integrin and Ku80 on naive CAC (empty bars), and after pretreatment with telbivudine (filled bars). UT7/Epo-S1 cells served as a positive control. B) Increased expression of B19V transcripts after Telbivudine pre-treatment in UT7/S1 cells and ECFC. Quantification of the B19V NS1, 11kDa, VP2 in UT//S1, and NS1 in ECFC after 2 h pretreatment with Telbivudine after B19V infection during 24 hours

normoxia, 24 hours hypoxia, 48 hours normoxia, and 48 hours hypoxia. C) Reduced B19V-induced apoptosis after Telbivudine pre-treatment in B19V-infected eo-EPC and ECFC. Quantification of active caspase-3 positive ECFC and eo-EPC after treatment with control plasma and control plasma + telbivudine (white bars), B19V infection (light grey bars) and 2 h pretreatment with Telbivudine before B19V infection. D) PCR Array for apoptosis and BIRC3 after Telbivudine pre-treatment in B19V-infected ECFC. (A) Regulation of apoptotic genes in ECFC; control plasma-treated with versus without Telbivudine pretreatment (blue bars), B19V-infected versus control plasma-treated (red bars), and B19V-infected with 2 h Telbivudine pretreatment versus control plasma-treated (green bars). (B) Quantification of BIRC active caspase-3 positive ECFC andeo-EPC after treatment with control plasma and telbivudine (white bars), B19V infection (light grey bars) and before B19V infection. Data are means +SD.

The data of our study show an effect of the nucleoside analogue Telbivudine on susceptibility of B19V infection of CAC with higher number of B19V replication intermediates and a striking anti-apoptotic action through normalisation of cIAP2 levels. These results extend the knowledge of activities of Telbivudine against known human viruses and show a novel anti-apoptotic action. Thus, Telbivudine may be an interesting candidate to unravel new insights of cellular mechanisms B19V infection.

In summary, we demonstrate CAC as targets for infection by B19V and causative agent for impaired endothelial regenerative capacity, thus challenging the established concept of B19V being responsible for a primary chronic organ disease. The thymidine analogon telbivudine improves clinical outcome in chronic myocarditis and reduces apoptosis in circulating angiogenic cells through stabilisation of CIAP-2 (BIRC 3) levels.

3.2.2 Project-related publications of the investigator(s)

1. **C. Schmidt-Lucke,** F. Spillmann, T. Bock, S. van Linthout, M. Meloni, U. Kühl, D. Lassner, H.-P. Schultheiss, C. Tschöpe. Interferon-beta modulates endothelial damage in patients with cardiac persistence of parvovirus B19. JID. 2010, March; 201: 936-945.
2. GP Fadini, Maruyama S, Ozaki T, Taguchi A, Meigs J, Dimmeler S, Zeiher A, de Kreutzenberg S, Avogaro A, Nickenig G, **C Schmidt-Lucke** , Werner N. Circulating progenitor cell count for cardiovascular risk stratification. A pooled analysis. PLoS ONE. 2010, Jul 9;5(7):e11488.
3. **Schmidt-Lucke, C,** S Fichtlscherer, A Aicher, C Tschöpe, H-P Schultheiss, A M Zeiher, S Dimmeler. Quantification of circulating endothelial progenitor cells using the modified ISHAGE protocol. PLoS ONE. 2010, 0013790
4. Van Linthout S, Savvatis K, Miteva K, Peng J, Ringe J, Warstat K, **Schmidt-Lucke C**, Sittinger M, Schultheiss HP, Tschöpe C. Mesenchymal stem cells improve murine acute coxsackievirus B3-induced myocarditis. Eur Heart J. 2011 Sep;32(17):2168-78.
5. Pozzuto T, von Kietzell K, Bock T, **Schmidt-Lucke C**, Poller W, Zobel T, Lassner D, Zeichhardt H, Weger S, Fechner H. Transactivation of human parvovirus B19 gene expression in endothelial cells by adenoviral helper functions.Virology. 2011 Mar 1;411(1):50-64.
6. **Schmidt-Lucke**, C, F Escher, S Van Linthout, K Miteva, J Peng,K Savvatis, U Kühl, D Lassner, H-P Schultheiss, C Tschöpe. Cardiac migration of endogenous mesenchymal stem cells in patients with inflammatory cardiomyopathy. 2. Revision.
7. Duechting A, **Tschöpe C,** Kaiser H, Lamkemeyer T, Tanaka N, Aberle S, Lang F, Torresi J, Kandolf R, Bock CT. Human parvovirus B19 NS1 protein modulates inflammatory signaling by activation of STAT3/PIAS3 in human endothelial cells. **J Virol.** 2008; 82: 7942-52.
8. Winter K, von Kietzell K, Heilbronn R, Pozzuto T, **Fechner H,** Weger S. Roles of E4orf6 and VA I RNA in adenovirus-mediated stimulation of human parvovirus B19 DNA replication and structural gene expression. J Virol. 2012, 86(9):5099-109.
9. Pinkert S, Klingel K, Lindig V, Dörner A, Zeichhardt H, Spiller OB, **Fechner H**. Virus-host coevolution in a persistently coxsackievirus B3-infected cardiomyocyte cell line. J Virol. 2011, 85(24):13409-19.

3.3 Funding

Funding of the project within the Collaborative Research Centre started July 2008. Funding of the project ended December 2013.

3.3.1 Project staff in the ending funding period

	No.	Name, academic degree, position	Field of research	Department of university or non-university institution	Commitment in hours/week	Category	Funded through:
Available							
Research staff	1	C. Schmidt-Lucke, MD, PI	Endothelial regeneration, B19V	Dept. of Cardiology and Pulmology, Charité Berlin	10		MEDIACC GmbH
Non-research staff	1	M. Sosnowski, technician		Dept. of Cardiology and Pulmology, Charité Berlin	39		External funding
Requested							
Research staff		Thomas Zobel, PhD, Postdoc	Virology	Dept. of Cardiology and Pulmology, Charité Berlin	39	Postdoc	
Non-research staff							

Job description of staff (supported through available funds):

1. Caroline Schmidt-Lucke, PD Dr. med. Responsible for project management, administration of the project, and reporting. Primary supervisor of the MD-students involved. Supervision of the technicians. Coordination of the experimental work (strategy and logistics), data analysis of expression studies. Preparation of tables and figures for publications and writing of manuscripts. She is funded by MEDIACC GmbH.

2. Marzena Sosnowski. Was working in the group since 2005 of the applicant Schmidt-Lucke and was primary responsible for the in vitro assays of infection and transfection of CAC. She was doing excellent work and has high skills with regards to cultivation conditions for CAC, infection and transfection of B19V, and required read-outs. She was indispensable for the successful progress of the experiments and requires her complete working time. She worked on the project until 7/2013.

Job description of staff (requested):

1. Thomas Zobel, Dr. rer. nat. was working in the group of C. Schmidt-Lucke since 2006. He was working in the field of molecular virology especially on mechanisms of damage of parvovirus B19 virus infection on angiogenetic cells. He has strong expertise in the design and execution of in vitro experiments and actively performed the experiments until 7/2013.